HOSTED BY

ELSEVIER

Available online at www.sciencedirect.com

ScienceDirect

Soils and Foundations 61 (2021) 1386–1398

www.elsevier.com/locate/sandf

Technical Paper

Assessment of the upstream slope failure of a dam due to repeated cyclic drawdown

Suttisak Soralump *, Kobid Panthi, Suriyon Prempramote

Department of Civil Engineering, Faculty of Engineering, Kasetsart University, Bangkok, Thailand

Received 16 August 2020; received in revised form 7 August 2021; accepted 13 August 2021
Available online 14 September 2021

Abstract

Khlong Pa Bon Dam in Thailand underwent the greatest differential drawdown in impounded water in 2014. Unexpected deformation of the upstream slope of the dam was observed on June 27 in the year, after operation for 10 years. The drawdown was hypothesized as the possible cause of the slope deformation. The results from piezometers showed that the upstream slope remained partially undrained after sudden drawdowns. A rapid drawdown analysis confirmed that the movement did not occur due to the sudden drawdown of water in 2014. Back analysis revealed that the shear strength of the embankment slope was near its residual value at the time of failure, which was validated by the movement of inclinometers. Ring shear tests were used to determine the residual shear strength of the failure zone, and the results were validated by the finite element method in ABAQUS. Furthermore, the results of the numerical analysis demonstrated that strain softening was the major cause of the slope movement.

Keywords: Slope movement; Site investigation; Strain accumulation; Rapid drawdown failure; Residual strength; Numerical modeling

1. Introduction

Rapid removal of water after a certain period of elevation such that the slope does not have sufficient time to drain the water is termed rapid drawdown (RDD). The stabilizing effect of water on the upstream slope of the embankment is lost, but the pore water pressure may remain high, depending on the permeability of the material during RDD (USBR 2011). Various studies have been carried out to analyze slope failures arising from RDD (Chen and Huang 2011; Alonso and Pinyol 2016; Archard 2016; Duncan, Wright, and Wong 1990; Moregenstern 1963; VandenBerge, Duncan, and Brandon 2013; Pinyol et al. 2011). In most cases, RDD failure occurred after years of operation of embankment structures that had undergone repeated water unloading–reloading cycles; however, none of these previous studies considered the possibility of strain softening of the soil as a result of the cyclic loading of water. The design criteria for multi-stage stability analysis during RDD also do not consider the cyclic impact of water on the embankment slope (USBR 2011). This study aims to investigate the cause of the upstream slope movement of the Khlong Pa Bon Dam using RDD analysis and numerical simulations of the strain softening due to cyclic loading of water.

Strain softening leads to progressive failure because of the reduction in shear strength with increasing strain and appears when the strength parameters are evaluated at very large strain levels (Chai and Carter 2009; Griffiths and Lane 1999; Potts, Kovacevic, and Vaughan 1997; Sterpi 1999; Troncone 2006). The cyclic load caused by the accumulation of shear strain causes a reduction in shear strength as a result of the cyclic sinusoidal loading and unloading of water (Chen, Zhang, and Chan 2018; Juneja

Peer review under responsibility of The Japanese Geotechnical Society.
* Corresponding author.
E-mail address: soralump_s@yahoo.com (S. Soralump).

https://doi.org/10.1016/j.sandf.2021.08.006
0038-0806/

and Mohammed Aslam 2016). The soil stiffness degrades along with the maximum shear stress with an increase in the volumetric strain due to the cyclic loading of water (Anderson and Eichart 1976; Sun, Indraratna, and Nimbalkar 2014; Koutsoftas 1978; Soralump and Prasomsri 2016; Thian and Lee 2018); however, there is some concern regarding whether this also occurs under smaller frequencies. During cyclic shearing, if the threshold cyclic shear strain is exceeded, a permanent volume change accumulates (Vuceic 1994). As a result, the materials exhibit a loss of strength from the peak to residual value at large strains, which leads to local failure (Skempton 1964).

The strain softening behavior of clays under undrained or partially drained conditions can be modeled using the modified cam clay (MCC) model (Chai and Carter 2009). This model has been successfully applied to problems involving the loading of clay samples or geotechnical construction on clay (Wood, 1990). The MCC model represents the soil in the over-consolidation state and is one of the best methods for representing the phenomenon of strain softening.

2. Background

Khlong Pa Bon Dam is a 45 m high embankment structure with a length of 750 m and a reservoir capacity of 20 million cubic meters (Soralump et al. 2019). The dam is laid on a granite rock foundation with an overburden soil consisting of impervious residual soil. The dam body consists of an impervious clay core, shell zone, boulder riprap, and filter material. The impervious clay core consists of low plastic clay (CL), whereas the shell zone consists of silty clay with gravel. Gravelly clay and sandy clay are present in the soil foundation. A chimney drain and blanket drain are included to allow drainage of water from the clay core and prevent the downstream slope from becoming saturated. The cross-section of the Khlong Pa Bon Dam is shown in Fig. 1.

Operation of the Khlong Pa Bon Dam began in 2004. On June 27, 2014, physical movement was observed at the upstream slope in three locations: 0 + 272, 0 + 297, 0 + 332 m and their vicinity (Fig. 2), and this movement has continued to the present date. The movement started from a higher elevation and is currently moving toward the dam toe. As the slope has continued to move each year since 2014, there is great concern regarding the safety of this dam in the future. Despite continuous movement, the dam is being operated with simple modifications each year by maintaining the drawdown height (Panthi and Soralump 2020).

In 2014, the dam underwent a drawdown of 24.22 m in 241 d, resulting in the lowest water level ever observed in the reservoir. It was hypothesized that this drawdown was the major cause of the upstream slope movement. During a site inspection, a vertical movement of 2 m was observed at the failure zone along the 80 m length (Fig. 2 and Fig. 3). In the hydrograph of Khlong Pa Bon Dam, it can be observed that the movement occurred when the water level was 96.45 m (Fig. 4), while no movement was observed in 2013 when the minimum water level was 93.13 m (Table 1). If the failure occurred due to RDD, this raises the important question of why no movement occurred in 2013. The drawdown of the water level in the Khlong Pa Bon Dam is summarized in Table 1.

3. Site investigation

Various site investigations were performed after the slope movement in 2014. Borehole investigations with depths of 8–10 m were carried out at the failure zone (i.e., 0 + 272 m, 0 + 297 m, and 0 + 332 m) in 2014, followed by another investigation near the toe zone in 2017 (Panthi and Soralump 2020). The probable failure surface identified from the borehole investigation is marked by the red section in Fig. 5. Similarly, echo sounding was conducted to investigate the extent of the slope movement in 2017 and 2020. The movement was observed from 0 + 272 m to 0 + 332 m and the vicinity in 2017, while movement from 0 + 260 to 0 + 380 m was observed in 2020, indicating that the failure section has been increasing each year (Fig. 6).

Additionally, an anomaly was distinctly visible around the failure zone in the electrical resistivity test; the presence of pore water pressure indicated that the slope was partially undrained (Fig. 5). The presence of water within the slope indicates the infiltration of water in the failure zone after the movement of the upstream slope. The results obtained from the resistivity test were consistent with the results obtained from the borehole investigation. In addition to these tests, spectral analysis of surface waves (SASW) was also performed along the crest. In most of the test positions, the shear wave velocity in the depth range of 20 m

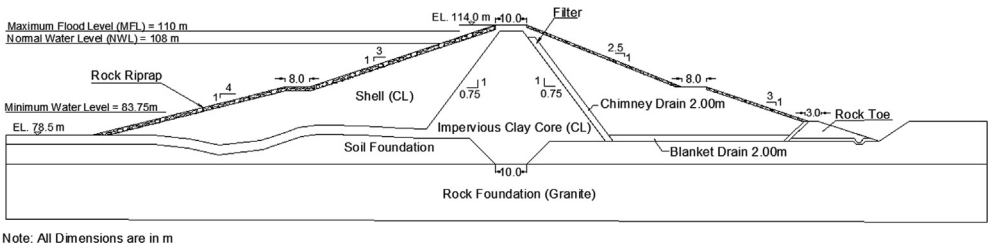

Fig. 1. Cross section of the Khlong Pa Bon Dam (0 + 297 m).

Fig. 2. Observation of a crack at the upstream slope of Khlong Pa Bon Dam (Royal Irrigation Department 2016).

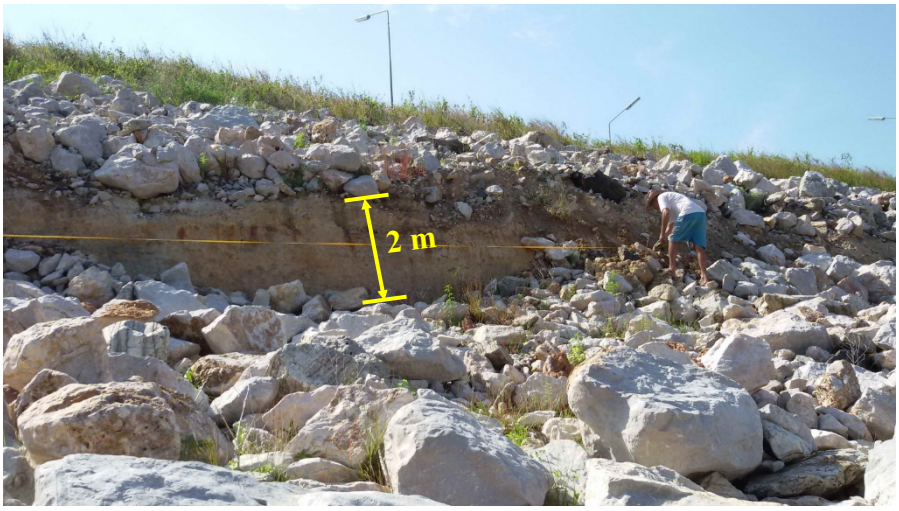

Fig. 3. Physical measurement of the upstream slope after the first movement (Royal Irrigation Department 2016).

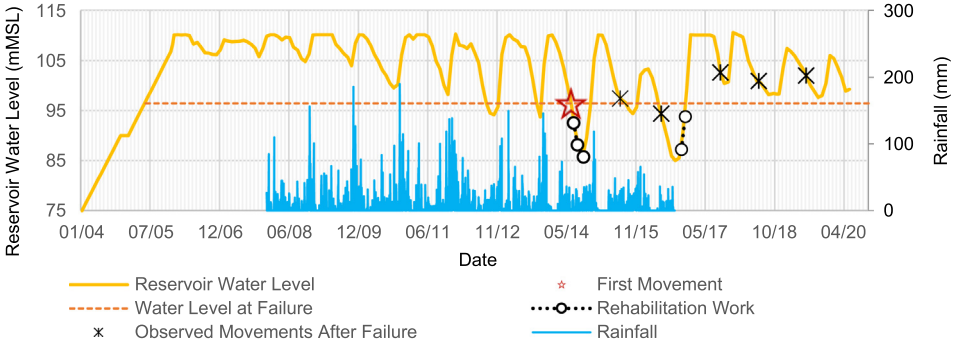

Fig. 4. Rainfall, hydrograph, and timeline of the Khlong Pa Bon Dam.

was approximately 200–400 m/s (Fig. 5), indicating that the embankment structure consisted of compacted soil layers. There was no significant difference between the results at the test positions near the area of movement and those outside the area of movement.

3.1. Inclinometer results

At the time of slope movement, no inclinometers were present in the failure zone. However, because the movement of the slope has continued each year, four inclinome-

Table 1
Data of water level drawdown of Khlong Pa Bon Dam (2004–2018).

Drawdown Year	Drawdown Date	Level (m)	Drawdown Height (m)	Rate of Drawdown (cm/d)
2006	5/23/06	110.09	4.21	2.24
	11/27/06	105.88		
2007	6/28/07	109.14	3.7	3.25
	10/20/07	105.44		
2008	7/1/08	109.65	5.27	4.02
	11/9/08	104.38		
2009	6/8/09	109.84	6.47	4.37
	11/3/09	103.37		
2010	1/4/10	110.27	10.89	4.24
	9/18/10	99.38		
2011	6/18/11	109.83	11.93	8.97
	10/29/11	97.9		
2012	6/11/12	107.6	14.31	11.27
	10/16/12	93.29		
2013	6/25/13	108.09	14.96	10.76
	11/11/13	93.13		
2014*	2/1/14	110.05	24.33	10.10
	9/30/14	85.72		
2015	1/6/15	110.13	15.92	5.47
	10/24/15	94.21		
2016	1/25/16	102.99	17.99	8.37
	8/27/16	85		
2017	6/14/17	110.09	6.67	9.01
	8/27/17	103.42		
2018	3/2/18	108.99	10.81	5.60
	9/11/18	98.18		

* First observation of movement at the Khlong Pa Bon Dam.

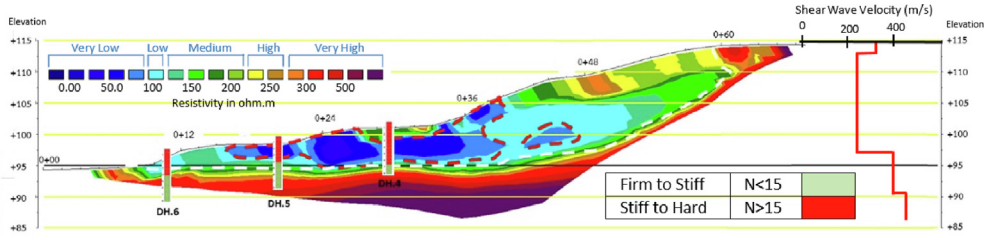

Fig. 5. Comparison of the results of resistivity tests, SASW, and borehole investigations (0 + 297 m).

ters were installed in December 2018 to observe the in situ movement of the upstream slope. There was no movement in the upstream slope with decreases in the water level until early May 2019, but movement was observed beginning in July 2019 when the water level was lowered by 5.5 m from the initial condition (Fig. 4 and Fig. 7). It was found that the observed movement was a continuation of the previous slope movement. The failure surface estimated from the various site investigation results is shown in Fig. 8.

4. Material properties

To investigate the failure mechanism, a number of laboratory tests were conducted on soil samples from the failure zone, downstream slope, borrow area, and stock pile. The soil index properties were determined based on Atterberg's limit, as detailed in Table 2. Additionally, the compressibility of the soil was determined from consolidation tests and was later used in the numerical analysis. Because the failure occurred after the rapid removal of water, a consolidated undrained (CU) triaxial test was conducted to simulate the undrained behavior of the slope. The strength parameters obtained from the various laboratory tests are listed in Table 3.

The investigation was based on the assumption that the strength of the soil was reduced from the peak to the residual value at the time of failure. Thus, the residual strength of the slope was determined from reversal direct shear tests (Fig. 9) and ring shear tests (Fig. 10). The normal stresses used in the laboratory tests ranged from 25 kPa to 300 kPa, which is within the normal stress range of the failure zone, i.e., 0–160 kPa. Laboratory tests were conducted to simulate the exact site conditions. The methods used for the reversal direct shear tests and ring shear tests were based on previous tests conducted by multiple researchers (Stark and Hussain 2010; Suzuki, Tsuzuki, and

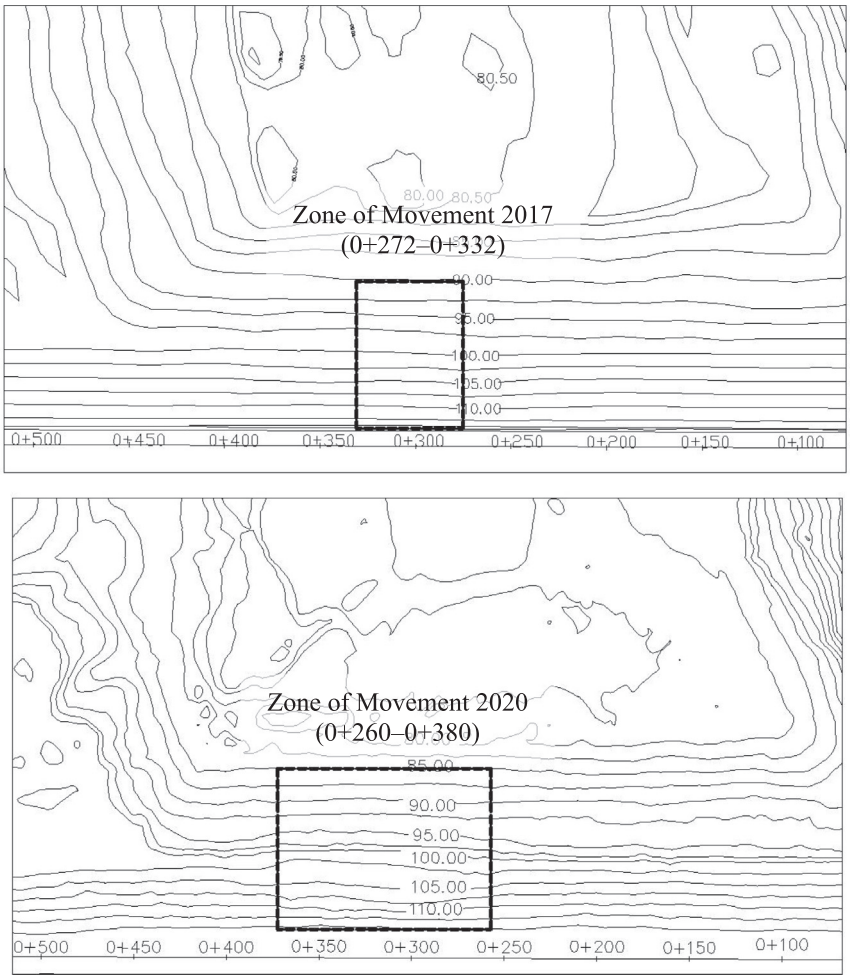

Fig. 6. Zones of movement identified using echo sounding (2017 and 2020).

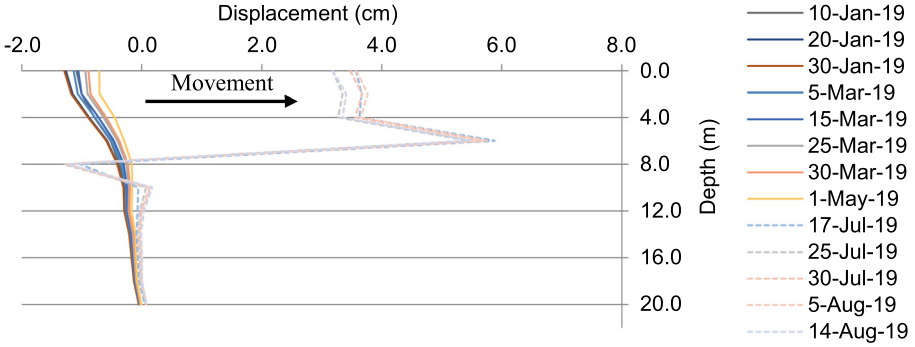

Fig. 7. Inclinometer results (IN4) at the Khlong Pa Bon Dam (Dec 15, 2018 to Aug 10, 2019).

Yamamoto 2005; Anayi, Boyce, and Rogers 1988; Head 2011).

5. Numerical modeling

A numerical model of the Khlong Pa Bon Dam was designed to investigate the behavior of the upstream slope with fluctuations in the water level. For the failure zone, all of the parameters used in the numerical analysis were determined from the laboratory tests, while the parameters of the clay core, rock riprap, filter, soil foundation, and rock foundation were obtained from the material properties used during the design of the embankment structure. The soil parameters used in the numerical analyses are listed in Table 4.

The 3D simulations of the ring shear tests using the MCC model were performed in ABAQUS, which is based on the finite element method (FEM). The objective of the

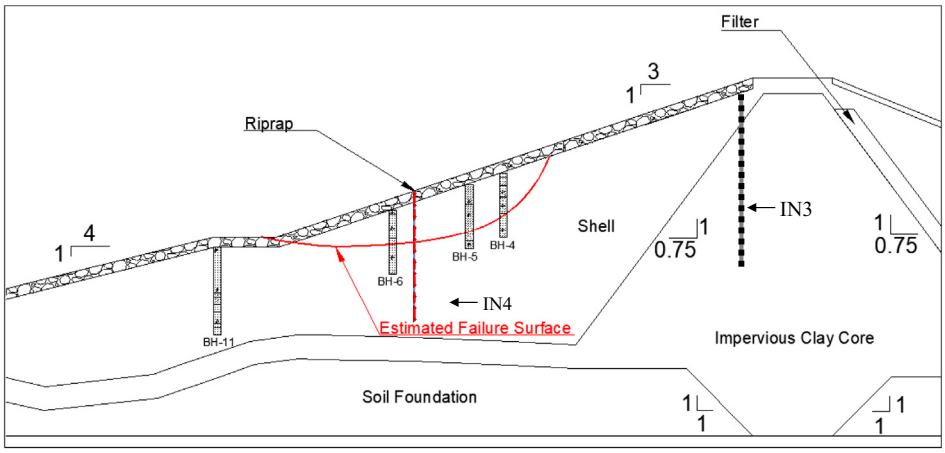

Fig. 8. Determination of the failure plane from site investigations.

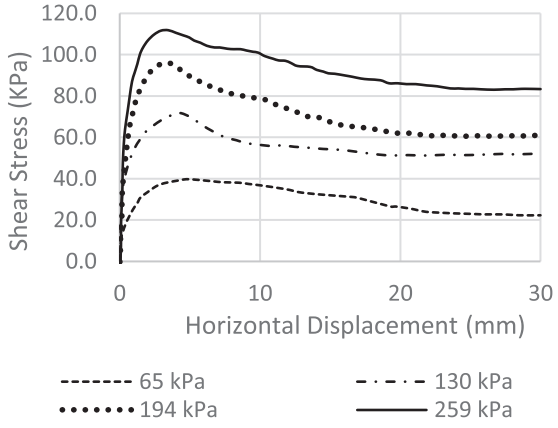

Fig. 9. Results of reversal direct shear tests on the failure slope.

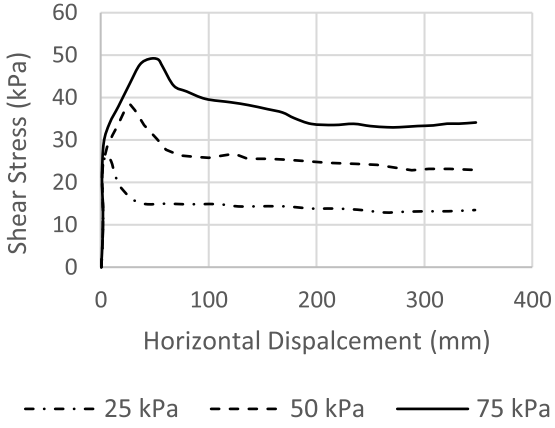

Fig. 10. Results of ring shear tests on the failure slope.

3D ring shear test simulation was to validate the residual shear strengths obtained from the ring shear tests. The input parameters used in the numerical model were based on the parameters used for the laboratory tests. A saturated sample model was used for the analysis with three different normal stresses (25 kPa, 50 kPa, and 75 kPa) under a

Table 2
Index properties of soil samples.

Properties	Failure Zone	Downstream Slope	Stock Pile	Borrow Area	Embankment Design
Gs	2.68	2.7	2.7	2.67	2.67
LL (%)	45	39	42	39	49
PL (%)	22.94	21.56	21.96	22.45	24
PI (%)	22.06	17.44	20.04	16.55	25
SL (%)	16.12	17.27	16.85	18.09	–
USCS Classification	CL	CL	CL	CL	CL

Table 3
Shear strength parameters of soil samples (failure zone).

S. No.	Soil Strength Parameter Test	c_{cu} (kPa)	Φ_{cu}	c' (kPa)	Φ'	c'_r (kPa)	Φ'_r
1	Material used for embankment construction (direct shear test)	–	–	19.1	18.42	–	–
2	Upstream slope (triaxial CU test)	14.25	15.83	21.72	17.52	–	–
3	Upstream slope (direct shear test)	–	–	20.01	20.36	1.03	17.45
4	Downstream slope (direct shear test)	–	–	18.93	19.24	0.67	17.63
5	Upstream slope (ring shear test)	–	–	15.1	24.09	1.9	22.87
6	Back analysis (failure zone)	–	–	5.1	17.82	–	–

Note: The subscripts 'cu' and 'r' denote the consolidated undrained test and residual strength, respectively.

Table 4
Soil parameters for the numerical analysis.

Material Properties	Shell Zone		Clay Core	Rock Riprap	Filter	Rock Toe	Soil Foundation	Rock Foundation
	MC Model	MCC Model						
Unit Weight (kN/m^3)	19	19	19.5	22	20	22	22	23.5
Permeability, k_x (m/d)	0.055	0.055	0.000378	86,400	4.58	86,400	0.0008	1.00E-06
Conductivity Ratio (ky/kx)	0.5	0.5	0.25	1	1	1	1	1
Young's Modulus (kPa)	13,520	–	20,480	75,000	35,000	50,000	20,000	65,000
Poisson's Ratio	0.39	0.39	0.32	0.2	0.25	0.2	0.32	0.3
Residual Cohesion (kPa)	0	0	20	0	0	0	0	–
Residual Angle of Internal Friction (°)	17.63	17.63	23	41	35	39	30	–
O.C. Ratio	–	3.75	–	–	–	–	–	–
Initial Void Ratio	–	0.885	–	–	–	–	–	–
Slope of Consolidation Line, λ	–	0.113	–	–	–	–	–	–
Slope of Swelling Line, κ	–	0.021	–	–	–	–	–	–

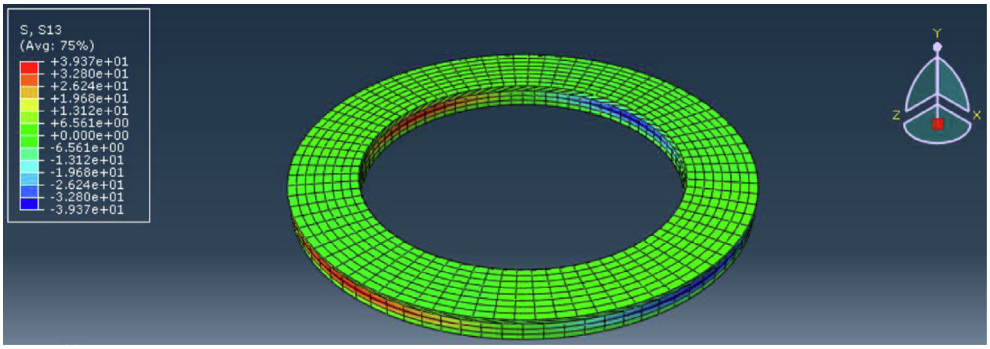

Fig. 11. 3D simulation of a ring shear test in ABAQUS.

shear rate of 0.25°/min. A 3D simulation of a ring shear test in ABAQUS is shown in Fig. 11.

The residual shear strengths obtained from the ring shear tests are compared with the results obtained from the FEM in ABAQUS in Table 5 and the results are also plotted in Fig. 12. The numerical analysis was conducted under the same conditions as those used in the laboratory test for a fair comparison. The results obtained from the FEM are in good agreement with the results of the laboratory tests, as shown in Fig. 12

Coupled analysis using FEM was employed to determine the stress distribution in the slope. SIGMA/W was coupled with SEEP/W for the generation and dissipation of pore water pressure in the soil in response to the change in water level to solve both the equilibrium and flow equations. Boundary conditions were defined in the foundation and lateral directions to stabilize the soil model. In the downstream zone, a boundary with a constant head and no seepage was used. In the upstream zone, two boundary conditions (i.e., the hydraulic boundary condition and stress/strain boundary condition) were used for the coupled stress analysis. The function for the water level variation was defined based on actual reservoir data.

Table 5
Residual shear strength results obtained from ring shear tests and FEM simulations.

Normal Stress (kPa)	Residual Shear Strength (kPa)	
	Ring shear test	FEM
25	13.08	12.6
50	21.94	24.78
75	34.18	39.37

5.1. Transient seepage analysis

Transient seepage analysis helps in the prediction of pore water pressure in embankments (Brahma and Harr 1963; Desai 1972; Browzin 1961) and the finite element program SEEP/W presents a method for using uncoupled transient seepage analysis (Stark et al. 2017). Transient seepage analysis was used to determine the flow of water in the embankment slope of the Khlong Pa Bon Dam.

The results from the transient seepage analysis were compared with results obtained from 14 standpipe piezometers located at 0 + 130 m. The instrumentation results for the total head from piezometer number 10 (PZ10) and SEEP/W for 2500 d to 5000 d are shown in Fig. 13. Because the permeability of the clay core is very low, no significant variation in the water level was observed in the piezometer with fluctuation of the water level. This behavior was observed for all of the piezometers installed in the clay core (Panthi and Soralump 2020). Furthermore,

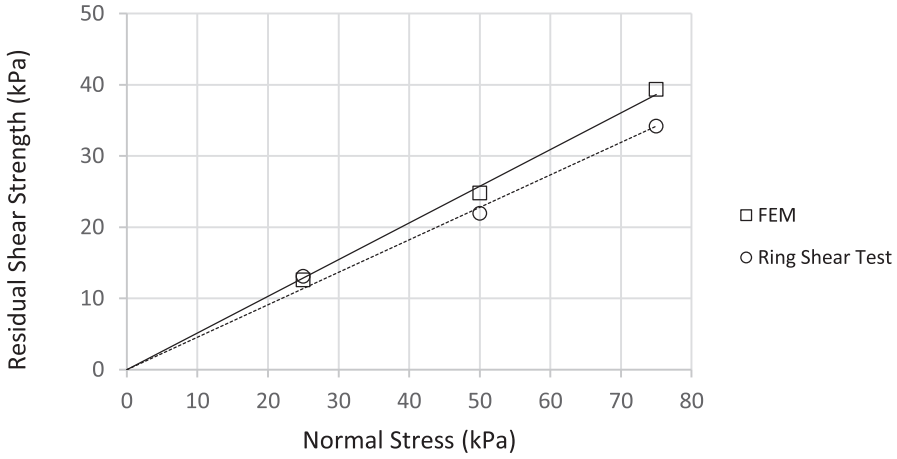

Fig. 12. Relationship between the residual shear strength and normal stress.

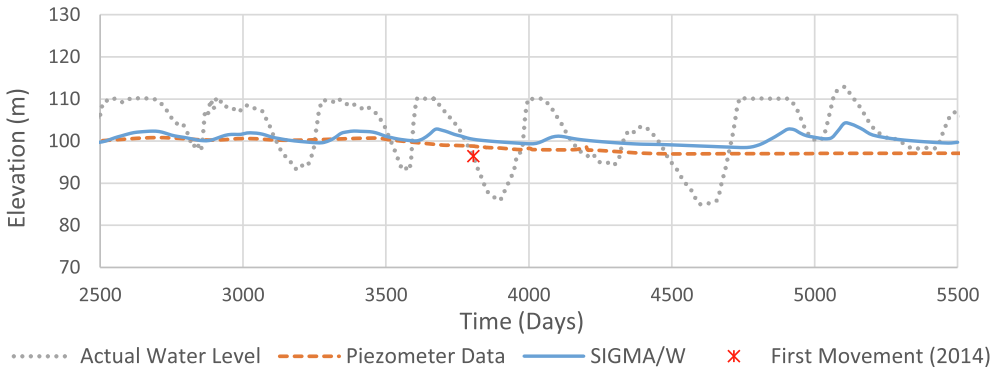

Fig. 13. Comparison of water levels: actual level, piezometer data, and SEEP/W results.

the total water head at the embankment on the 3894th day (minimum water level) from the date of impounding shows that the results obtained from the piezometer and SEEP/W are almost identical (Fig. 14). It was found that the slope was partially undrained after each drawdown.

5.2. Rapid drawdown analysis

RDD analysis was performed in the failure zone (0 + 297 m) to determine the behavior of the slope after the rapid removal of water in 2014. The undrained shear strength parameters obtained from the CU test were used in this analysis (Table 3). The equation proposed by Duncan can be used to determine the dissipation of excess pore water from the slope (Duncan, Wright, and Brandon 2014), as follows:

$$T = \frac{c_v t}{d^2} \tag{1}$$

where c_v is the coefficient of consolidation (m^2/y);

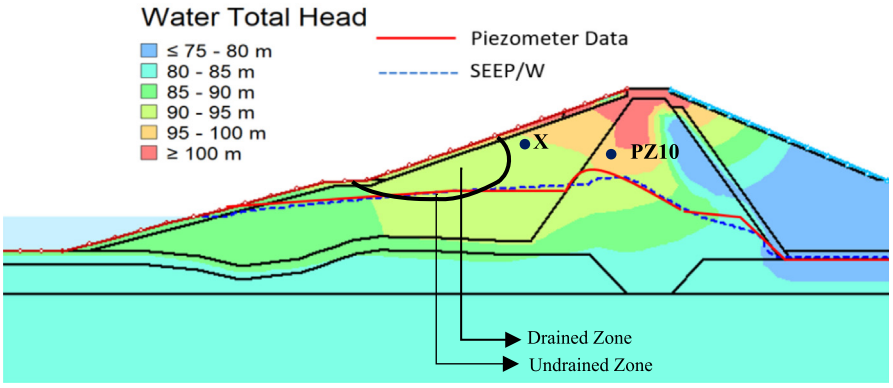

Fig. 14. Comparison of water levels obtained from the piezometer data and SEEP/W for 0 + 297 m (3894 d).

t is the time for the drawdown of water (y);
d is the length of the drainage path (m);
T is the time factor.

If $T \geq 3$, the dissipation of pore water pressure during drawdown will be at least 90%, and the material can be treated as fully drained; if $T < 3$, the dissipation of pore water pressure will be less than 90%, and the soil is treated as undrained (Duncan, Wright, and Brandon 2014). After the rapid removal of water from Khlong Pa Bon Dam in 2014, the slope was found to be in an undrained condition ($T = 2.04$).

5.2.1. Rapid drawdown using the FEM strength reduction method and DWW method

The strength reduction technique can be used to determine the FoS during rapid drawdown of water (Griffiths and Lane 1999). Similarly, based on two well-documented case histories, the empirical factor, R, for strength reduction during rapid drawdown was found to be 70 (VandenBerge, Duncan, and Brandon 2013) and the adjusted undrained shear strength can be expressed as follows:

$$s_{u-ADJ} = \left(\frac{R}{100}\right) s_{u-CIU} \tag{2}$$

where

$S_{u\text{-}ADJ}$ is the adjusted undrained strength;
$S_{u\text{-}CIU}$ is the undrained shear strength measured in the laboratory (19.105 kPa);
R is the empirical strength reduction factor.

The FoS of the Khlong Pa Bon Dam was obtained using an R of 70, as presented in Table 6. Similarly, an analysis was also carried out with PLAXIS using the c-phi reduction technique. The c-phi reduction was performed using a procedure of load advancement with a number of steps. Furthermore, the method proposed by Duncan, Wright, and Wong (DWW method) was used to determine the factor of safety for RDD analysis (Duncan, Wright, and Wong 1990). This analysis was performed using SLOPE/W. The FoS predicted by the FEM strength reduction method and DWW method are presented in Table 6. The FoS obtained from the different methods were greater than one, indicating that the failure did not occur as a result of the RDD.

5.3. Factor of safety with drawdown of water

The relationship between the drawdown of water levels and FoS is shown in Fig. 15 for the peak and residual strengths. The FoS initially decreases with the decrease in water level, then remains constant after a certain drawdown elevation, and finally starts to increase again. The characteristics of the relationship between the drawdown elevation and FoS are consistent with the results obtained in previous research (Zheng et al. 2009). At the failure zone, the FoS was minimum when the water level ranged from 92 to 98 m. This is termed the critical range of the water. The upstream slope movement in 2014 was observed when the water level was within this critical range (Fig. 15).

The in situ results obtained from the inclinometers showed that the upstream slope started moving in 2019 when the water level was lowered by 5.5 m (Fig. 7). Similarly, the slope stability analysis using the residual strength parameters also showed that the FoS was less than 1 when the drawdown elevation was less than 105 m from MSL (5 m in the case of Khlong Pa Bon Dam). Therefore, the results obtained from the inclinometer and slope stability

Table 6
Comparison of the factors of safety obtained with different analysis methods.

Analysis method	Factor of safety (FoS)
Finite element strength reduction method (PLAXIS)	1.258
Strength reduction (Vandenberge et al. 2013)	1.340
DWW method (Duncan, Wright, and Wong 1990)	1.250

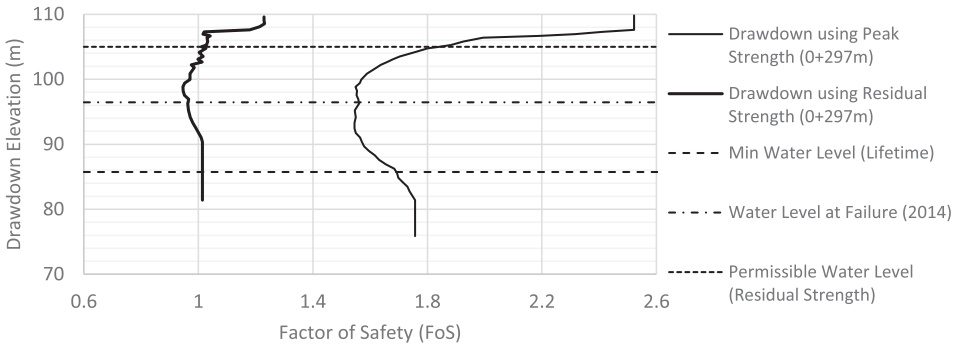

Fig. 15. Variation in the factor of safety with the drawdown level based on the peak and residual strengths.

analyses confirm the assumption that the shear strength of the slope was from the peak to residual value after the first slope movement in 2014 and reached the residual strength in 2019.

The concept of the drawdown factor was used in this analysis to separate the elastic and plastic zones. The depth from the impounding level to the point with the minimum FoS (Fig. 15) is defined as the yield drawdown elevation. This elevation corresponds to the point at which the soil supposedly surpasses the elastic limit and starts to yield. The drawdown factor (the ratio of the total drawdown elevation to the yield drawdown elevation) is used to define the water level that separates the elastic and plastic zones. The plot of the relationship between the drawdown factor and the number of cycles shows that the soil surpasses the elastic state when the drawdown factor is greater than one (Fig. 16), and strains start to accumulate from that year onward. The major limitation of this analysis is that it cannot determine the phase when the soil surpasses the peak strength but has not yet reached the residual strength. Hence, the design considering the drawdown factor is very conservative.

5.4. Analysis under cyclic loading of water

The Khlong Pa Bon dam undergoes cyclic unloading–reloading of water each year. The over-consolidation ratio (OCR) for the saturated soil of the upstream slope is 3.75. Based on the principle of the critical state model (CSM), heavily over-consolidated clays (OCR > 2) during drained and undrained conditions will undergo strain softening, and the value of shear stress will decrease at higher strains (Budhu 2013). Therefore, this analysis was based on the hypothesis that the upstream slope underwent strain softening due to the cyclic loading of water.

The shear stresses obtained from the reversal direct shear tests were compared with the results obtained from the MCC model with the passage of time at the failure zone. A normal stress of 65 kPa was applied to the soil sample obtained from the failure zone to determine the residual shear strength (Fig. 9). Furthermore, the shear stress was determined at point X (Fig. 14) from the numerical analysis with a normal stress of 65 kPa and compared with the result obtained from the direct shear test (Fig. 17). The results show a reduction in shear stress in both the lab-

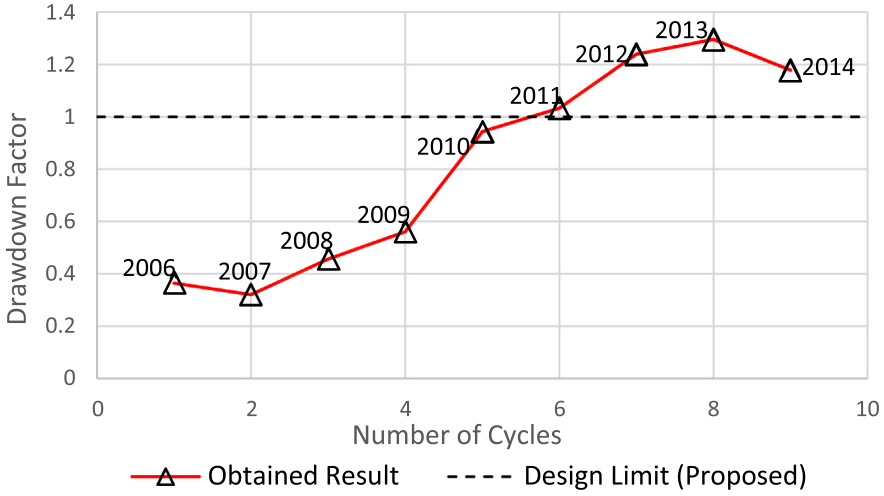

Fig. 16. Variation in the drawdown factor with the number of cycles for Khlong Pa Bon Dam.

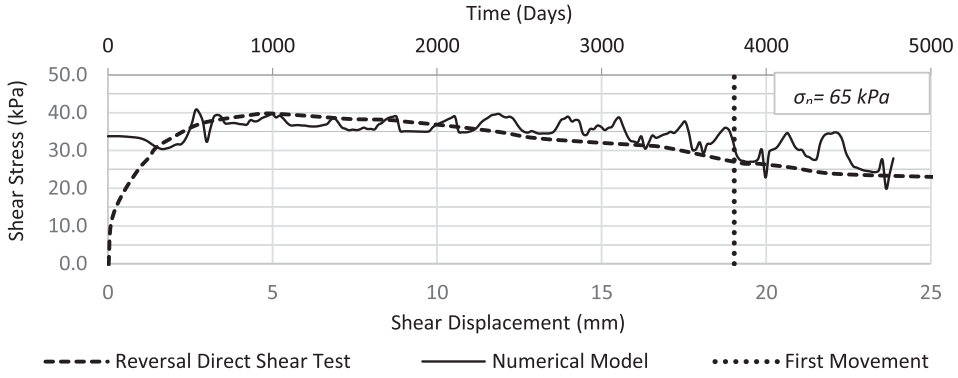

Fig. 17. Comparison of shear stresses obtained in the laboratory tests and numerical modeling.

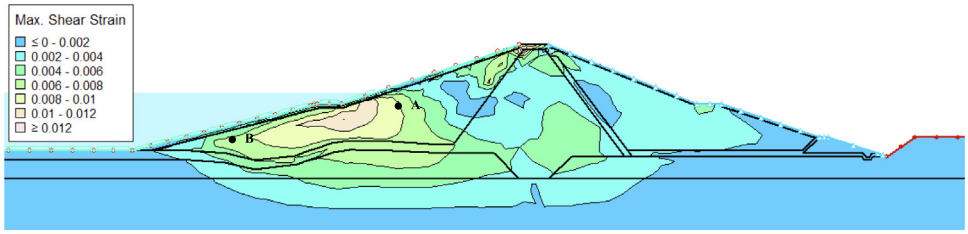

(a)

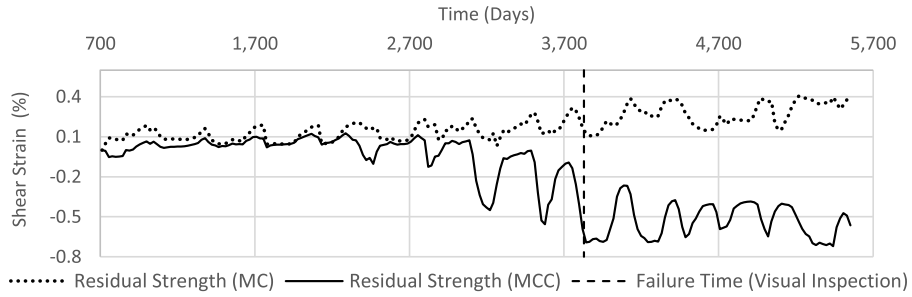

(b)

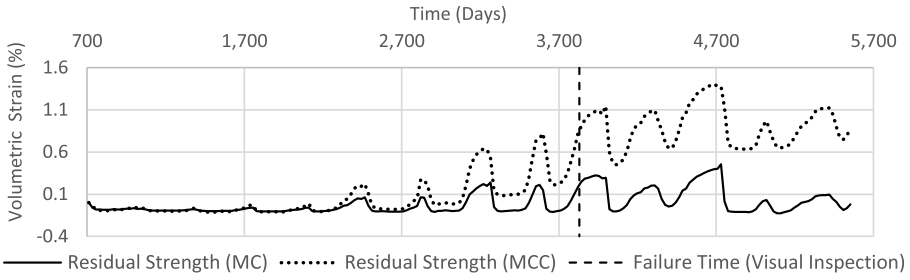

(c)

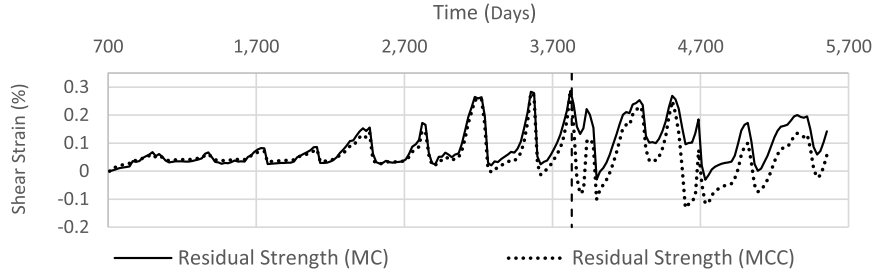

(d)

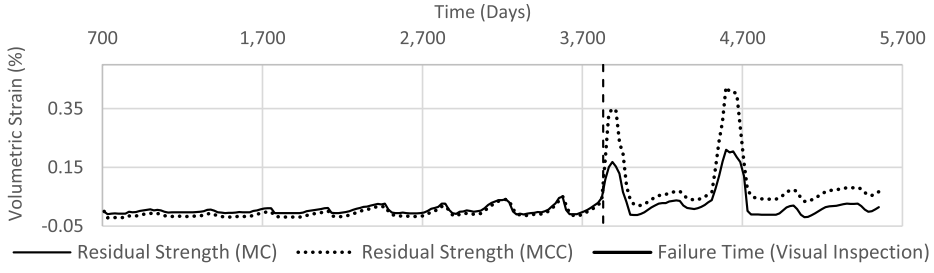

(e)

Fig. 18. (a) Maximum shear strain contours of the dam section at 0 + 297 m at 3820 d; (b) shear strain time history curve at the failure zone (Point A); (c) volumetric strain time history curve at the failure zone (Point A); (d) shear strain time history curve at a non-failure zone (Point B); (e) volumetric strain time history curve at a non-failure zone (Point B).

oratory test and numerical analysis, and the trends of curves obtained from the two analyses are similar. This result serves to verify the numerical model and confirm that shear stress was reduced due to fluctuations in the water level. Therefore, a numerical model was used to determine the softening behavior of the upstream slope.

5.5. Finite element analysis of strain softening

The failure of the embankment slope showed some unusual behavior that could not be resolved with the current design standards. Therefore, the MCC model was used to determine the strain softening behavior of the slope, and the results were compared with those of the conventional MC model. The MC model defines failure as the attainment of the maximum stress, but the failure stress state may not be sufficient to guarantee failure.

The maximum shear strain contour of the dam section at 0 + 297 m is shown in Fig. 18(a), where point A is located in the zone of movement and point B is located in a zone where no movement was observed. The values of the shear and volumetric strains were normalized after the first impounding. In the failure zone, the MC model showed an increase in both shear and volumetric strain with the drawdown of water, but the original state was reached after one complete cycle (Fig. 18(b) and (d)). In contrast, an accumulation of both volumetric strain (1%) and shear strain (0.7%) was observed in the MCC model (Fig. 18(b) and (d)). The results obtained from this model are consistent with the experiments conducted by Chen et al. (Chen, Zhang, and Chan 2018). Likewise, no major accumulation of shear or volumetric strain was observed at Point B (Fig. 18(c) and (e)) with either model because the zone was always saturated and was less affected by the water level fluctuation. It was found that the fluctuation of the water level was directly proportional to the accumulation of shear and volumetric strain. The results also show that the MC model cannot determine the softening behavior of the slope; therefore, the current design standard in Thailand cannot ensure the safety of the embankment slope.

The stress–strain curve was also plotted at the failure zone to investigate the behavior of the upstream slope with fluctuations in the water level (Fig. 19). The plot of the relationship between the maximum total stress and maximum shear strain was obtained from the numerical model at point X (Fig. 14). The results show that the upstream slope was in the elastic phase from 2004 to 2010 (Point P) because the shear strain returned to its original state after each drawdown cycle. However, after 2010, the soil surpassed the elastic phase, leading to the accumulation of shear strain (Point Q). With each additional drawdown cycle, the strain accumulated, causing movement of the slope in 2014. The strain –time history curve shows that the strain began to accumulate (Fig. 18) when the drawdown factor was greater than one (Fig. 16).

5.6. Conclusion and recommendations

The upstream slope movement of the Khlong Pa Bon Dam was investigated in this study. Results from inclinometers and various site investigations were used to confirm the location and depth of the failure plane, which was then applied in the numerical analysis. Furthermore, results from the piezometer and transient seepage analyses indicated that the slope was partially undrained after the rapid removal of water in 2014. An RDD analysis was performed to determine the behavior of the slope after the rapid removal of water. The results from the RDD analysis revealed that the failure did not occur as the result of a single rapid drawdown, and the slope did not fail due to the rapid removal of water. The results raise questions regarding the current design standard used in Thailand. From the back analysis, a reduction in the shear strength of the upstream slope was observed at the time of failure. Therefore, the MCC model was used to investigate the softening behavior of the upstream slope. The shear stress results obtained from laboratory tests and numerical analyses were used to validate the numerical model.

The Khlong Pa Bon Dam experienced significant drawdown for three consecutive years (2012–2014) following two smaller drawdowns (2010–2011). The piezometer results also showed that the slope was partially undrained during this period (Fig. 13). Therefore, the shear strength of the soil surpassed the peak strength during these drawdown cycles, changing the soil from the elastic to plastic phase. Furthermore, strain accumulation was also observed after the soil had surpassed the peak strength.

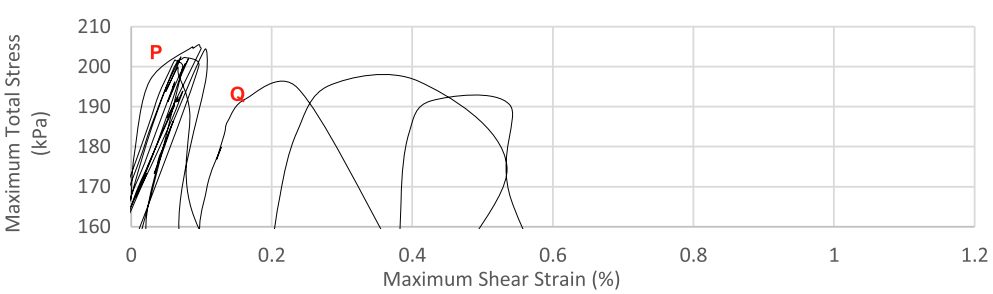

Fig. 19. Stress–strain curve at the failure section (Point X) for Khlong Pa Bon Dam.

Acknowledgements

The authors would like to thank the Geotechnical Engineering Research and Development Center (GERD), Kasetsart University for funding this research and the Royal Irrigation Department, Thailand for providing site investigation data.

Reference

Alonso, E.E., Pinyol, N.M., 2016. Numerical analysis of rapid drawdown: applications in real cases. Water Sci. Eng. 9 (3), 175–182. https://doi.org/10.1016/j.wse.2016.11.003.

Anayi, J.T., Boyce, J.R., Rogers, C.D.F., 1988. Comparison of alternative methods of measuring the residual strength of a clay. Transp. Res. Rec. 1192, 16–26.

Anderson, D.G., Eichart, F.E., 1976. Effects of straining on shear modulus of clays. ASCE J. Geotech. Eng. 102 (9), 975–987.

Archard, Michael Steven, 2016. Finite element analysis of embankment dam due to rapid drawdown events. Massachusetts Institute of Technology.

Brahma, S.P., Harr, M.E., 1963. Transient development of the free surface in homogenous earth dam. Geotechnique 12 (4), 283–302.

Browzin, B.S., 1961. Nonsteady-State Flow in Homogenous Earth Dams after Rapid Drawdown. Paper presented at the 5th ICSMFE, Paris.

Budhu, Muni, 2013. Soil Mechanics and Foundations. 3rd ed. United States of America: John Whiley and Sons, Inc.

Chai, J., Carter, J.P., 2009. Simulation of the progressive failure of an embankment on soft soil. Comput. Geotech. 36 (6), 1024–1038. https://doi.org/10.1016/j.compgeo.2009.03.010.

Chen, X., Huang, J., 2011. Stability analysis of bank slope under conditions of reservoir impounding and rapid drawdown. J. Rock Mech. Geotech. Eng. 3, 429–437. https://doi.org/10.3724/SP.J.1235.2011.00429.

Chen, Y., Zhang, G., Chan, D., 2018. Cyclic response and modeling of saturated silty clay due to fluctuations in reservoir water level of the Three Gorges Dam, China. Soils Found. 58 (3), 702–715. https://doi.org/10.1016/j.sandf.2018.02.023.

Desai, C.S., 1972. Seepage analysis of earth banks under drawdown. J. Soil Mech. Found. Div. 98 (11), 1143–1162.

Duncan, J.M., Wright, S.G., Brandon, T.L., 2014. Soil Strength and Slope Stability. Wiley, United States of America.

Duncan, J.M., Wright, S.G., Wong, K.S.. 1990. Slope Stability During Rapid Drawdown. Paper presented at the Seed Memorial Symposium Proceedings, Vancouver.

Griffiths, D.V., Lane, P.A., 1999. Slope stability analysis by finite elements. Géotechnique 51 (7):653–4. doi: 10.1680/geot.2001.51.7.653.

Head, K.H., 2011. Manual of Soil Laboratory Testing Volume 2: Permeability, Shear Strength and Compressibility tests. Third ed: Whittles Publishing.

Juneja, A., Mohammed Aslam, A.K., 2016. Strain accumulation in soils due to repeated sinusoidal loading. Jap. Geotech. Soc. Spec. Publicat. 2 (24), 903–906. https://doi.org/10.3208/jgssp.IND-18.

Koutsoftas, D.C., 1978. Effect of cyclic loads on undrained strength of two marine clays. ASCE J. Soil Mech. Foundat. Div. 104 (5), 609–620.

Moregenstern, N., 1963. Stability charts for earth slopes during rapid drawdown. Géotechnique 13 (2), 121–131.

Panthi, K., Soralump, S., 2020. Estimation of Failure Surface of Pa Bon Dam from Site Investigation. Jordan J. Civil Eng. 14 (1).

Pinyol, N.M., Alonso, E.E., Corominas, J., Moya, J., 2011. Canelles landslide: modelling rapid drawdown and fast potential sliding. Landslides 9 (1), 33–51. https://doi.org/10.1007/s10346-011-0264-x.

Potts, D.M., Kovacevic, N., Vaughan, P.R., 1997. Delayed collapse of cut slopes in stiff clay. Geotechnique 47 (5), 953–982.

Royal Irrigation Department, RID, 2016. Study the displacement behavior to improve Khlong Pa Bon dam. Phatthalung Province (in Thai).

Skempton, A.W., 1964. Long term stability of clay slopes. Geotechnique 14 (2):77–110.

Soralump, Suttisak, Pien-wej, Noppadol, Panthi, Kobid, Sanmuang, Jirawut, 2019. Cyclic drawdown of water causing the slope failure of canal and dam. Paper presented at the 16th Asian Regional Conference on Soil Mechanics and Geotechnical Engineering.

Soralump, Suttisak, Prasomsri, Jitrakon, 2016. Cyclic pore water pressure generation and stiffness degradation in compacted clays. J. Geotech. Geoenviron. Eng. 142 (1), 04015060. https://doi.org/10.1061/(ASCE)GT.1943-5606.0001364.

Stark, T.D., Hussain, M., 2010. Shear strength in preexisting landslides. J. Geotech. Geoenviron. Eng. 136 (7), 957–962. https://doi.org/10.1061/(Asce)Gt.1943-5606.0000308.

Stark, Timothy D., Jafari, Navid H., Zhindon, J. Sebastian Lopez, Baghdady, Ahmed, 2017. Unsaturated and transient seepage analysis of San Luis Dam. J. Geotech. Geoenviron. Eng. 143 (2), 04016093. https://doi.org/10.1061/(ASCE)GT.1943-5606.0001602.

Sterpi, Donatella, 1999. An analysis of geotechnical problems involving strain softening effects. Int. J. Num. Anal. Methods Geomech. 23 (13), 1427–1454.

Sun, Q.D., Indraratna, B., Nimbalkar, S., 2014. Effect of cyclic loading frequency on the permanent deformation and degradation of railway ballast. Géotechnique 64 (9), 746–751. https://doi.org/10.1680/geot.14.T.015.

Suzuki, Motoyuki, Tsuzuki, Shunsuke, Yamamoto, Tetsuro, 2005. Physical and chemical index property of residual strength of various soils. Memoris Facul. Eng. Yamaguchi University 56 (1), 1–11.

Thian, S.Y., Lee, C.Y., 2018. Shear strength degradation behavior of offshore clay under cyclic loading. Soil Mech. Found. Eng. 54 (6), 430–435. https://doi.org/10.1007/s11204-018-9492-6.

Troncone, A., 2006. Numerical analysis of a landslide in soils with strain-softening behaviour. Geotechnique 55 (8), 555–596.

USBR. 2011. Design Standards No. 13 Embankment Dams (Chapter 4: Static Stability Analysis Phase 4), Chapter 4: Static Stability Analysis Phase 4(Final): U.S. Department of the Interior Bureau of Reclamation.

VandenBerge, D.R., J.M. Duncan, T.L. Brandon, 2013. Rapid Drawdown Analysis using Strength Reduction. Paper presented at the International Conference on Soil Mechanics and Geotechnical Engineering, Paris.

Vucetic, Mladen, 1994. Cyclic threshold shear strains in soils. J. Geotech. Eng. 120 (12), 2208–2228.

Wood, David Muir, 1990. Soil Behaviour and Critical State Soil Mechanics. Cambridge University Press.

Zheng, Yingren, Tang, Xiaosong, Zhao, Shangyi, Deng, Chujian, Lei, Wenjie, 2009. Strength reduction and step-loading finite element approaches in geotechnical engineering. J. Rock Mech. Geotech. Eng. 1 (1), 21–30. https://doi.org/10.3724/sp.J.1235.2009.00021.